START PAGE

Chapter 13

PRACTICAL ISSUES WITH PWM CONVERTER MOTOR DRIVES

13.1. INTRODUCTION

Induction (IM), permanent magnet AC (PM-SM), reluctance synchronous (RSM) and switched reluctance (SRM) motors are brushless multiphase motors fed through PWM voltage-source converters (PECs) with bipolar and, respectively (for SRM), unipolar current capability. In all these drives, the line side converter is (still), in general, a diode rectifier with a DC link filter capacitor.

Also, the motors are fed through a cable of notable length (sometimes up to some hundreds of meters), with ultrafast voltage pulses (1-3μs or less in most cases). What are the effects of such drives on the motor itself and on the environment?

Let us enumerate a few of them:

- additional motor losses due to current and flux harmonics;
- current harmonics injected in the AC power supply (supply filter is necessary);
- electromagnetic interference due to the rather high switching frequency (up to 20kHz with IGBTs, in the hundreds of kW power range per unit);
- high frequency leakage currents' influence on motor current control and on circuit breakers;
- overvoltages along the stator coils first turns due to wave reflections of the PWM converter (special filters are required); these overvoltages are magnified by long cables;
- the steep-front voltage pulses produce both electromagnetic and electrostatic stray currents (voltages) in the bearings causing wear unless special measures are taken.

All these issues are called practical as they occur in industry where these drives are used every day for many hours.

13.2. THE BASIC PWM CONVERTER DRIVE

A basic PWM inverter drive with AC motors (or with SRMs) is made of a PEC, a power cable and the motor (Figure 13.1).

As variable speed drives are applied in various industries, the environment (thermal or chemical), the distance between the motor and the PEC, and the load cycle varies widely with the application. Variable speed drives may be introduced as new systems (the PEC and the motor) or the old

motor (IM or SM) — designed for sine wave supply — is not changed but rerated for the PEC supply and the new speed control range.

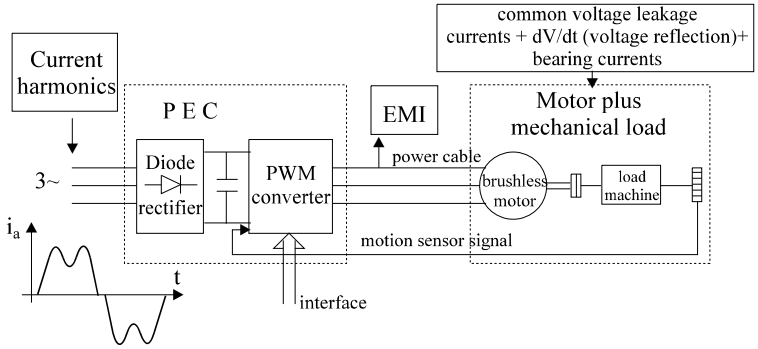

Figure 13.1. Basic PWM converter drive

Current harmonics in the power supply in the presence of the diode rectifier, long cable effects on voltage reflection (and dV/dt) at motor terminals, bearing currents and leakage currents are all consequences of the short rise time of voltage pulses in the PWM converter.

13.3. LINE CURRENT HARMONICS

Increasing the use of PWM converter drives for pumps, blowers, fans, and other industrial applications may lead to a notable infusion of current harmonics in the industrial systems.

A few questions arise:

- are harmonics filters needed?
- what type of filters (5^{th}, 7^{th}, 11^{th}, 13^{th} or combinations of these) are required?
- how to design (size) such filters?

Six-pulse PWM converters with diode rectifiers on the power system side draw harmonic currents of orders 5, 7, 11, 13, 17. In principle, each PEC has its own distinct harmonic signature.

The harmonic factor HF to define this signature is

$$HF = \frac{\sqrt{\sum_{5,7,11,\ldots} \nu^2 I_\nu^2}}{I_1} \tag{13.1}$$

The HF depends on the fact that the PWM converter is fed from a single-phase or three-phase supply, with or without line reactors, with or without an isolation transformer. HF varies in the interval 2 to 4% for three-phase supplies and up to 12% for single-phase AC supplies, for powers up to 400kW or more and IGBTs as SRCs.

The harmonic factor HF is related to the total harmonic distortion (THD) by

$$\text{THD} = \text{HF} \cdot \frac{\text{Drive kVA}}{\text{SC kVA}} \cdot 100\% \tag{13.2}$$

where drive kVA is the drive rated kVA and SC kVA is the short-circuit kVA of the power system at the point of drive connection.

In general, a 5% THD is required (IEEE-519-1992 and IEC 1000-3-2(3) standard). If this constraint is met, no line filter is needed. However, in general, this is not the case and a filter is necessary.

Harmonics filters consist of several sections of single (or double) tuned series L-C resonant circuits (Figure 13.2).

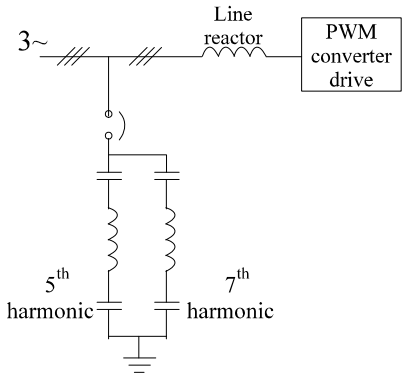

Figure 13.2. Line filters

Separate filters for each drive above 15kW are advisable but aggregate filters for multidrive nodes may also be used, especially if not all drives are working at full load most of the time.

Slightly below the resonance frequency (0.95), series LC filters behave like a capacitor and their design for this situation avoids the possibility of parallel resonance due to component parameter change because of temperature or aging.

The resonance frequency of a single tuned filter f_r is

$$f_r = \frac{1}{2\pi\sqrt{LC}}; \quad \alpha = \frac{f_r}{f_n} \tag{13.3}$$

α - detuning factor, f_n - nominal resonance frequency of the filter $f_n = \nu f_1$.

The filter impedance for ν^{th} harmonic, $Z_f(\nu)$, is,

$$\underline{Z}_f(\nu) = R_f + j\left[2\pi f_1 \nu L - 1/\left(2\pi f_1 \nu C\right)\right] \tag{13.4}$$

The filter capacitor reactive power kVAF (three-phase) for 60Hz is

$$\text{kVAF} = 2\pi f_1 10^{-3} C V_{LL}{}^2 = 0.3777 C V_{LL}{}^2 \tag{13.5}$$

where V_{LL} is the line voltage (rms) and C is in farads. The filter capacitor kVA is about (25-30%) of drive kVA rating. A harmonic filter attenuates all harmonic voltages at the point of connection but maximum attenuation occurs for frequencies close to its resonance frequency.

The attenuation factor $a_v(h)$ is

$$a_v(h) = \frac{V(h)}{V_f(h)} \tag{13.6}$$

$$V(h) = \%I(h) \cdot h \cdot (\text{Drive kVA} / \text{SC kVA}) \tag{13.7}$$

V(h) is the h harmonics voltage without the filter and $V_f(h)$ is with the ν^{th} order filter.

Neglecting the filter resistance

$$a_v(h) = \left(1 + \frac{(\nu\alpha)^2}{1 - (\nu\alpha / h)^2}\right) \frac{\text{kVAF}}{\text{SC kVA}} \tag{13.8}$$

In general, $a_v(h)$ should be higher than 1.0 to provide some attenuation.

The THD has to be limited for the voltage harmonics making use of V(h) of (13.7) for finding $V_f(h)$.

The filter is designed such that the THD is less than 5%. The allowed current THD may increase with the short-circuit ratio R_{sc} at the point of connection [2] from 5% for ($R_{sc} \le 20$) to 20% for $R_{sc} > 1000$

$$R_{sc} = \frac{\text{utility maximum short - circuit current}}{\text{maximum demand fundamental current}} \tag{13.9}$$

For a 5th-order harmonic current filter, the drive current waveform changes notably (Figure 13.3d).

The peak current is increased but continuous current conduction is obtained by eliminating the 5th current harmonic.

Designing adequate line filters for a local power industrial system with more than one PWM converter drive is a rather complex problem whose solution also depends on the power source impedance, through the short-circuit current ratio Rsc or through the drive kVA / SC kVA.

As the relative power of PWM converter drives is increasing and the power quality standards are more and more challenging, it seems that the trend is to provide each drive with its line filter to comply with some strict regulations.

Common point of connection filter additions may be made in “hot” PWM converter-drive zones with weak local power supplies.

In PWM converters we included both, the voltage source inverters for AC motor drives, and the multiphase choppers for SRM drives.

Line voltage instabilities in the presence of line filters with some fast (direct torque and flux - DTFC) control systems of AC motor drives [3] and with DC chopper-fed motor drives [4] have been reported. This aspect has to be taken care of when the drive with incorporated line filter is designed and built.

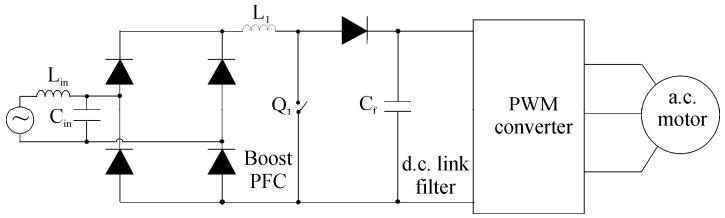

(a)

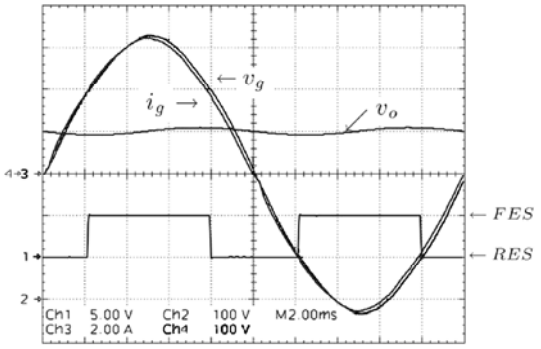

(b)

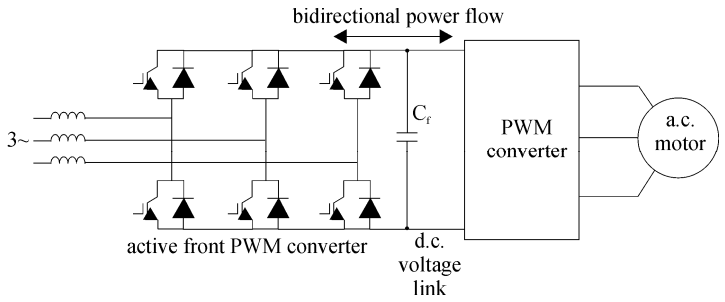

(c)

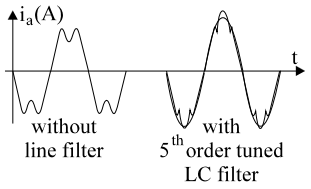

(d)

Figure 13.3. The boost PFC: a) the configuration, b) the obtained input voltage and current, c) the active front rectifier, d) 5th harmonic filtered in input current

Example 13.1. Line filter sizing

Let us consider that a PWM converter IM drive of 100kVA is connected to a local power system with a short-circuit power SC kVA = 1000kVA. The line current 5th, 7th and 11th harmonics are $i_5 = 0.15I_1$, $I_7 = 0.03I_1$, $I_{11} = 0.01I_1$; line frequency $f_1 = 60$Hz, line voltage $V_{LL} = 440$V (rms).

Calculate:

- the line current harmonic factor HF;
- the total distortion factor THD for the current;
- the filter capacitor C tuned to the 5th harmonic with $\alpha = 0.95$ (detuning factor), and the corresponding inductance L_f;
- the voltage attenuation factors $a_5(h)$ for the 5th, 7th and 11th harmonics;
- the voltage total harmonic distortion factor THD with the filter off and on.

Solution:

According to (13.1), HF is

$$HF = \frac{\sqrt{\sum_{5,7,11} \nu^2 I_\nu^2}}{I_1} = \sqrt{(5\cdot 0.15)^2 + (7\cdot 0.03)^2 + (11\cdot 0.01)^2} = 0.7865 \tag{13.10}$$

From (13.2) the THD current is

$$THD = HF \cdot \frac{\text{Drive kVA}}{\text{SC kVA}} \cdot 100\% = 0.7865 \cdot \frac{100}{1000} \cdot 100\% = 7.865\% \tag{13.11}$$

As THD is higher than the 5% recommended for drive kVA / SC kVA = 1/10, a line filter is required.

The filter is tuned to the 5th harmonic with $\alpha = 0.95$, so, from (13.3)

$$LC = \frac{1}{4\pi^2 (f_n \alpha \nu)^2} = \frac{1}{4\pi^2 (60\cdot 0.95\cdot 5)^2} = \frac{0.1308\cdot 10^{-6}}{25} s^2 \tag{13.12}$$

Also, the capacitor kVA is

$$\text{kVAF} = 0.3 \cdot \text{Drive kVA} = 0.3 \cdot 100 = 30\,\text{kVA} \tag{13.13}$$

From (13.5) C is

$$C = \frac{\text{kVAF}}{0.377 \cdot V_{LL}{}^2} = \frac{30}{0.377 \cdot 440^2} = 411 \cdot 10^{-6}\,\text{F} = 411\,\mu\text{F} \tag{13.14}$$

The harmonic voltage V(h) (with filter off) in the power source (in %) is found from (13.7)

$$\begin{aligned} V(5) &= \%\big(I(5)\big) \cdot 5 \cdot \frac{100}{1000} = 15 \cdot 5 \cdot \frac{100}{1000} = 7.5\ \% \\ V(5) &= \%\big(I(7)\big) \cdot 7 \cdot \frac{100}{1000} = 3 \cdot 7 \cdot \frac{100}{1000} = 2.1\ \% \\ V(5) &= \%\big(I(11)\big) \cdot 11 \cdot \frac{100}{1000} = 1 \cdot 11 \cdot \frac{100}{1000} = 1.1\ \% \end{aligned} \tag{13.15}$$

We may calculate the voltage THD before filtering

$$\begin{aligned} \text{THD}(\%) &= \sqrt{\big(5 \cdot V(5)\big)^2 + \big(7 \cdot V(7)\big)^2 + \big(11 \cdot V(11)\big)^2} = \\ &= \sqrt{(5 \cdot 7.5)^2 + (7 \cdot 2.1)^2 + (11 \cdot 1.1)^2} = 42.056\ \% \end{aligned} \tag{13.16}$$

The voltage attenuation factors are

$$\begin{aligned} a_5(5) &= \left(1 + \frac{(5 \cdot 0.95)^2}{1 - (5 \cdot 0.95/5)^2}\right)\frac{0.3}{10} = 6.942 \\ a_5(7) &= \left(1 + \frac{(5 \cdot 0.95)^2}{1 - (5 \cdot 0.95/7)^2}\right)\frac{0.3}{10} = 1.2845 \\ a_5(11) &= \left(1 + \frac{(5 \cdot 0.95)^2}{1 - (5 \cdot 0.95/11)^2}\right)\frac{0.3}{10} = 0.862 \end{aligned} \tag{13.17}$$

Based on the definition of $a_v(h)$, (13.6), we may calculate $V_f(5)$, $V_f(7)$, $V_f(11)$ and thus, from (13.1), the new voltage, THD_f (with the filter on) is

$$\begin{aligned} \text{THD}_f &= \sqrt{\big(5 \cdot V(5)/a_5(5)\big)^2 + \big(7 \cdot V(7)/a_5(7)\big)^2 + \big(11 \cdot V(11)/a_5(11)\big)^2} = \\ &= \sqrt{(5 \cdot 7.5/6.942)^2 + (7 \cdot 2.1/1.284)^2 + (11 \cdot 1.1/0.862)^2} = 18.66\ \% \end{aligned} \tag{13.18}$$

The beneficial effect of the 5th-order harmonic filter is only partly evident: a reduction of voltage THD from 42% to 18.66%. Note that in our example the 7th and 11th current harmonics were exaggerated and this

explains why the final value of THD_f is not much smaller (eventually below 8%). Also, the short-circuit power of the local grid was unusually small. An increase in the SC kVA of the local grid would improve the results.

Apart from passive input filters, hybrid (active-passive) filters may be used to compensate the input current and voltage harmonics and eventually deal with short voltage sags in the AC source.

The boost power factor correcter (PFC) is a typical such device (Figure 13.3a), applied for single phase AC source. [18, 20]

The boost PFC converter operates in continuous conduction mode. This way, with a proper control, the sinusoidal input current is reconstructed in phase with the AC source voltage (Fig. 13.3b). [18]

Also for input current filtering and unity power factor, the active front end rectifier-inverter (Fig. 13.3c) may replace the diode rectifier plus the passive input filter [21 - 23].

The active front end PWM converter provides quite a few functions:

- Stabilizes the AC link voltage "against" limited overload or against AC source short-lived voltage sags (three phase, two phase, single phase);
- Produces rather sinusoidal current input with limited current, controllable, power factor angle.
- Provides for fully bidirectional power flow, so needed for fast braking drives (such as in elevators).

13.4. LONG MOTOR POWER CABLES: VOLTAGE REFLECTION AND ATTENUATION

In many new and retrofit industrial applications the PWM converter and motor must be placed in separate locations, and thus long motor cables are required. The high rate of voltage rise (dV/dt) of up to 6000V/μs, typical for IGBT inverters, has adverse effects on motor insulation and produces electrostatic-caused currents in the bearings. The distributed nature of the long cable L-C parameters results in overvoltages which further stress the motor insulation. In addition, voltage reflection of the long cable is dependent on inverter pulse rise time (t_r = 0.1 to 5μs) and on the cable length which behaves like a transmission line.

PWM voltage pulses travel along the power cable at about half light speed (U^* = 150-200m/μs) and, if the pulses take longer than one third the rise time to travel from converter to motor, full reflection occurs; the voltage pulse level is doubled at motor terminals.

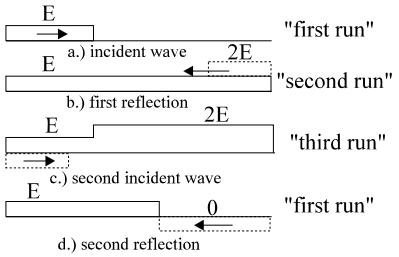

Figure 13.4. Reflection wave cycle

Let us consider a finite length cable with an infinite dV/dt voltage wave (pulse) traveling from converter to motor. The motor represents a high impedance with respect to such fast voltage pulses. The motor behaves like an equivalent uncharged capacitor in this case. Upon arrival, the incident wave is reflected (the capacitor charges). The reflected plus incident wave doubles the voltage at motor terminals (2E). The line is thus charged at 2E while at the sending end, the inverter output voltage is still E. Hence a −E (negative reflection) wave now travels from inverter to motor and thus, finally, the motor voltage becomes again E after three "runs" along the cable length (Figure 13.4). This is why it is said that, if the pulses take longer than one third of rise time to travel from inverter to motor, the reflected voltage is 2E at the motor terminals.

We may thus calculate the ideal peak line to line voltage V_{LL} at the motor terminals as [5,6]

$$V_{LL} = \begin{cases} \dfrac{3l_c \cdot E}{U^* \cdot t_r} \cdot \Gamma_m + E; & \text{for } t_{travel} < t_r / 3 \\ E \cdot \Gamma_m + E; & \text{for } t_{travel} > t_r / 3 \end{cases} \tag{13.19}$$

where Γ_m is the motor realistic reflection coefficient derived from transmission line theory

$$\Gamma_m = \frac{Z_{motor} - Z_{0c}}{Z_{motor} + Z_{0c}} \tag{13.20}$$

where Z_{motor} is the motor equivalent impedance and Z_{0c} is the surge impedance of the cable (of length l_c)

$$Z_{0c} = \sqrt{\frac{L_c}{C_c}} \tag{13.21}$$

A similar reflection coefficient Γ_c may be defined on the PWM converter output side. In the qualitative analysis in Figure 13.4, $Z_{motor} = \infty$ and, thus, $\Gamma_m = 1$. In reality, the motor impedance is more than 10-100 times larger than Z_{0c} and thus $\Gamma_m \cong 1$.

For $\Gamma_m = 1$, to reduce the overvoltage to almost zero, $t_{travel} < t_r / 3$ and thus

$$\frac{3l_c \cdot E}{U^* \cdot t_r} \cdot \Gamma_m \le 0.2E \tag{13.22}$$

Equation (13.22) provides a condition to calculate the critical cable length l_c above which virtual voltage doubling occurs. For E = 650V DC bus (480V AC system), $\Gamma_m = 0.9$, $U^* = 165\text{m}/\mu\text{s}$, from (13.22) we obtain

$$\frac{3l_c \cdot E}{U^* \cdot t_r} \cdot \Gamma_m = E \tag{13.23}$$

$$l_c = \frac{U^* \cdot t_r}{3\Gamma_m} = \frac{165}{3 \cdot 0.9} \cdot t_r = \left(61.11 \cdot t_r[\mu s]\right) \text{ meters} \tag{13.24}$$

Five times shorter cables in comparison with the critical length l_c (Figure 13.5) are required to reduce the motor overvoltage to 20% (13.22). This latter condition may not be met in many applications.

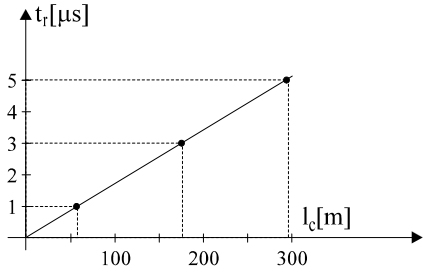

Figure 13.5. Voltage rising time t_r versus critical cable length

For long cables, the solution is to reduce the reflection coefficients at motor side $\Gamma_m(Z_m)$ (13.20) and on converter output side $\Gamma_c(Z_c)$. This may be done by adding a filter at motor terminals, for example, to reduce Z_m (Figure 13.6). Consequently, a low pass filter at converter output will increase the voltage pulse rise time which has the effect of allowing cables longer than l_c (Figure 13.6b).

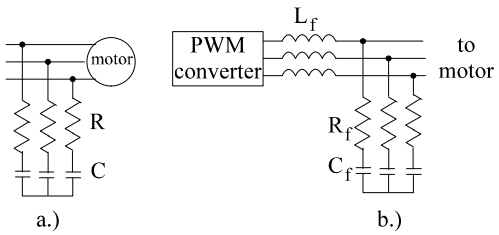

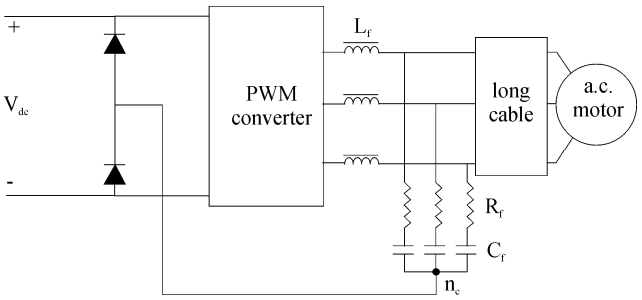

c.)

Figure 13.6. First-order filters: a.) at motor terminals, b.) at PWM converter output, c) LRC filter with diode clamp

According to [6] the total voltage across the R-C motor terminal filter, E_r, is

$$E_r = 2E\left(1 - \frac{Z_{0c}}{R + Z_{0c}} e^{-\frac{t}{(R+Z_{0c})C}}\right); \quad R = Z_{0c} \tag{13.25}$$

To design the filter, we may limit E_r to $E_r = 1.2E_0$ (20% overvoltage) for $t = t_r$ (rising time)

$$1.2E = 2E\left(1 - \frac{Z_{0c}}{R + Z_{0c}} e^{-\frac{t_r}{2Z_{0c}C}}\right) \tag{13.26}$$

Thus we may calculate the filter capacitor C while the resistance $R = Z_{0c}$ (Z_{0c} — the cable surge impedance).

On the other hand, the influence of inverter output low pass filter is materialized by a voltage delay

$$V(t) = E\left(1 - e^{-\frac{t_r}{\tau}}\right) \tag{13.27}$$

$$\tau = \sqrt{L_f C_f} \tag{13.28}$$

where τ is the filter time constant. Evidently,

$$\tau \geq t_r \tag{13.29}$$

The capacitor has to be chosen as $C_f > l_c.10^{-10}$ (F): L_f is obtained from (13.28) with τ imposed and the resistance R_f is calculated assuming an overdamped circuit

$$R_f \geq \sqrt{\frac{4L_f}{C_f}} \tag{13.30}$$

Typical results with a motor terminal filter and inverter output filter are given in Figure 13.7a and b, respectively.

Note: Increase in the rise time of the terminal voltage may impede the control system performance in the motor parameter identification (for tuning) mode. Care must be exercised when designing the drive to account for this aspect.

Recently, overvoltages (above the doubling effect of ideal reflection) of up to 3 times the DC link voltage E have been reported in connection with some PWM patterns which, once modified adequately by pulse elimination techniques, lead to lowering the ideal overvoltage to twice the value of E [7].

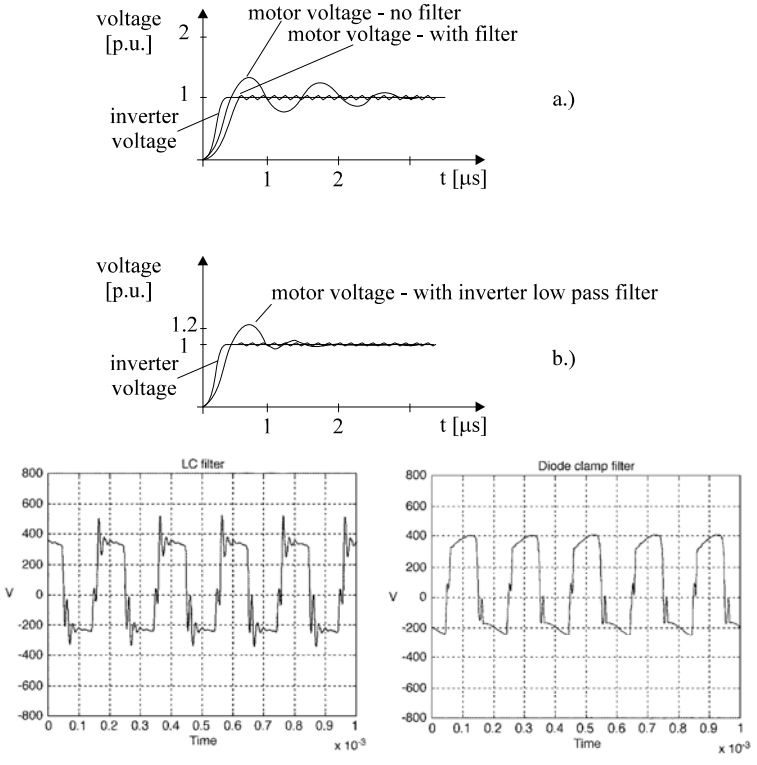

Figure 13.7. Motor terminal voltage: a.) with motor terminal RC filter, b.) with inverter low pass filter, c) 2.2 kW induction motor with low pass filter L_f = 2.6 mH, C_f = 1.4 μF, d) 2.2 kW induction motor with low pass filter L_f = 2.6 mH, C_f

= 1.4 μF and diode clamp

A rather low cost solution to reduce drastically motor terminal overvoltage due to high dV/dt and their propagation along motor cable (as shown earlier in this paragraph) adds to the differential LRC filter (Fig. 13.6c) two diodes in the DC link whose middle point is connected to the capacitors null point (Fig. 13.6c) [24].

The LC filter still operates in the differential mode to reduce dV/dt but the diode-clamp occurs whenever an overvoltage due to ringing is present. When the capacitor null point n_c voltage becomes larger than $\pm V_{dc}/2$ the corresponding diode (upper or lower) starts conducting; this way the DC link voltage is clamped. For a 2.2 kW drive, L_f = 2.6 mH, C_f = 1.4 μF would be suitable [24].

The simulated motor terminal voltage at 8 kHz fundamental frequency with f_{sw} = 4.5 kHz switching frequency (Fig. 13.7c, d) for the LRC filter without and with diode-clamping shows a 15 to 20 % further reduction of motor terminal overvoltage with the diode-clamp. Experiments fully confirmed these results [24].

Medium and large IM still experience failures in their windings due to voltage sources (high dV/dt and overvoltage) [25]. Attributing these failures to winding insulation weakness or to cable length and type (fully shielded or only bundled) or to PWM strategy in the converter is not always straightforward and a comprehensive study is required to find the actual cause.

Adding an LC filter with diode clamp looks like a fairly practical solution to the problem, especially when the existing motor is kept and only the inverter drive is added anew.

13.5. MOTOR MODEL FOR ULTRAHIGH FREQUENCY

For the fast rising voltage pulses produced by the PWM at the motor terminals, the motor behaves like a complex net of self and mutual inductances and capacitors between winding turns C_s and between them and earth C_p (series parallel) — Figure 13.8.

Besides the stator model (Figure 13.8), the rotor windings (if any) have to be added. Owing to the presence of parallel capacitors C_p and $C_{p1,2}$ the voltage pulse at the motor terminals (a, b, c), in the first nanoseconds, is not uniformly distributed along the winding length. Thus, even if neutral n of the stator windings is isolated, the first coils of windings have to withstand more than (60-70%) of the voltage pulse. Consequently, they are heavily stressed and their insulation may wear out quickly. Increasing the voltage rise time at motor terminals reduces this electrostatic stress and thus even existing line-start motors may work with PWM converter drives for a long time.

It is also possible to use special thin insulation for motor windings and/or use random windings to distribute the initial voltage pulse with high dV/dt randomly through the winding.

13.6. COMMON MODE VOLTAGE: MOTOR MODEL AND CONSEQUENCES

The structure of a PWM inverter drive is shown in Figure 13.9.

Assume that the zero sequence impedance of the load (motor) is Z_0. The zero sequence voltage V_0 is

$$V_0 = \frac{V_{an} + V_{bn} + V_{cn}}{3} = \frac{V_a + V_b + V_c}{3} - V_n \tag{13.31}$$

and

$$i_0 = \frac{i_a + i_b + i_c}{3} \tag{13.32}$$

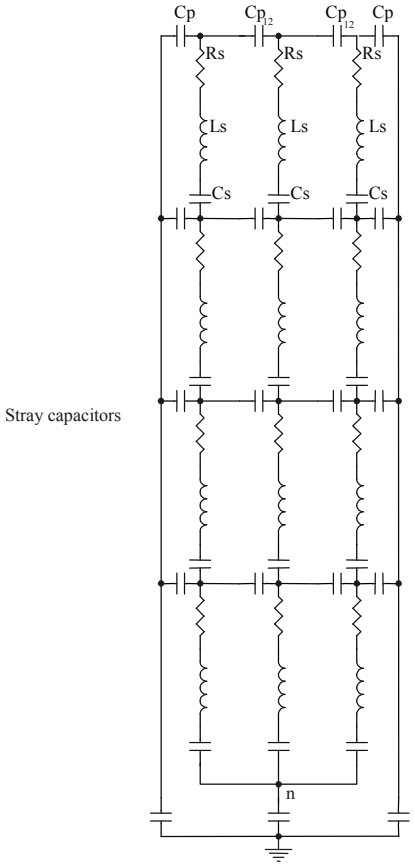

Figure 13.8. Motor RLC equivalent circuit for superhigh frequencies

(stator only considered)

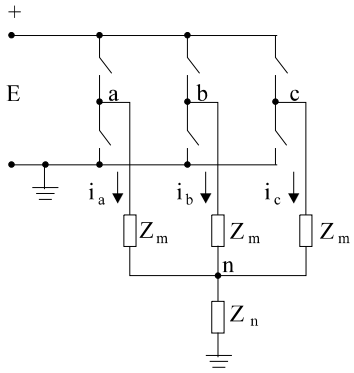

Figure 13.9. PWM inverter with motor and common mode impedance Z_n (isolated null point)

The relationship between V_0 and i_0 is:

$$V_0 = Z_0 i_0 \tag{13.33}$$

Consequently, common mode current i_n and common mode voltage at neutral point V_n are:

$$i_n = i_a + i_b + i_c = \frac{3}{Z_0 + 3Z_n} \frac{V_a + V_b + V_c}{3} \tag{13.34}$$

$$V_n = \frac{3Z_n}{Z_0 + 3Z_n} \frac{V_a + V_b + V_c}{3} \tag{13.35}$$

As known, the common current mode is decoupled from the differential current mode (the balanced phase impedance Z_m is not involved).

Consequently, the equivalent common mode input voltage V_{oin} is

$$V_{0in} = \frac{V_a + V_b + V_c}{3} \tag{13.36}$$

and the machine impedance is as in (13.34) and Figure 13.10

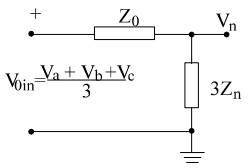

Figure 13.10. Motor model for common mode input voltage

For each commutation sequence in the converter, the common mode input voltage V_{oin} varies with E/3 approximately (E – DC link voltage). To the quick common voltage pulses, the motor behaves like stray capacitors between stator windings and stator laminations in parallel with capacitors through the airgap to the shaft and in parallel with capacitors from the null point through bearings to the common grounding point (Figure 13.11) [8,9].

Let us note that the power cable, common mode choke (to be detailed later) and line reactors may be represented as common voltage series and parallel impedances Z_s, Z_p between the inverter and the motor.

Also, the $3Z_n$ impedance may be replaced by capacitors and by the equivalent circuit of the voltage of the rotor shaft to ground V_{rg} (Figure 13.11).

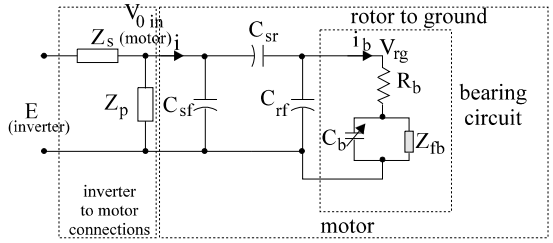

Figure 13.11. Common mode motor model for high frequencies

The bearing is represented by the bearing resistance (R_b), in series with a capacitor C_b which is in parallel with a nonlinear impedance Z_{fb} representing the intermittent shorting of capacitance C_b through bearing film breaking by the voltage pulses.

C_{sr} - equivalent capacitor from stator to rotor;

C_{sf} - equivalent capacitor between stator and frame;

C_{rf} - equivalent capacitor between rotor laminations and frame.

It now becomes evident that any voltage pulse from the inverter, when a switching in the inverter takes place, also produces a common mode voltage V_{oin} of E/3. This common voltage pulse results in a high common mode leakage current i_n. If large, this common mode (leakage) current can influence the null protection system. Reducing i_n means implicitly to reduce the shaft voltage V_{rg} and the bearing noncirculating current i_b [9]. Though $i_b << i_n$, it manages to deteriorate the bearings through the breakdown of lubricant film.

We will first deal with the stator common mode (leakage) current i_n which, in some cases, may be as large as the rated current.

13.7. COMMON MODE (LEAKAGE) STATOR CURRENT REDUCTION

As we are, for the time being, interested only in the leakage current $i_l(t)$, we may lump the motor and cable through a series RLC circuit whose components may be determined experimentally (Figure 13.12) by applying a

pulse from the converter and measuring the leakage current i_l, which looks like that in Figure 13.12.b.

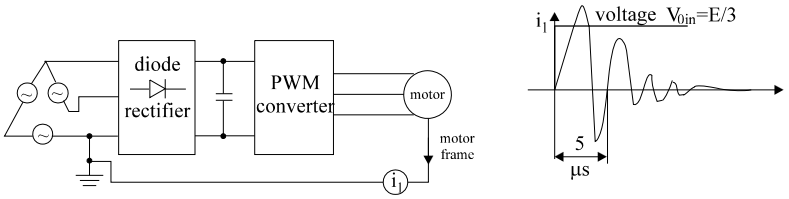

Figure 13.12. Measuring the leakage current: a.) test circuit, b.) current response to step voltage

The leakage current response resembles that of an RLC circuit. L is related to the cable inductance, C is the stray capacitance between windings and frame and R is related to the motor only.

After adding a common mode choke L_c at motor terminals (Figure 13.13.a), we obtain an equivalent circuit as in Figure 13.13b.

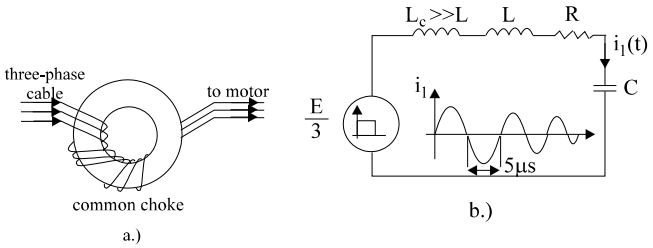

Figure 13.13. Common mode choke: a.) equivalent circuit, b.) leakage current $i_l(t)$

The peak leakage current is notably reduced (Figure 13.13b) by the presence of the common mode choke but the rms value is still not drastically reduced.

Placing a secondary coil (connected to a resistor R_t) on the common choke core [10] (Figure 13.14a.) has proved to drastically reduce both peak and rms leakage current values (Figure 13.14.b).

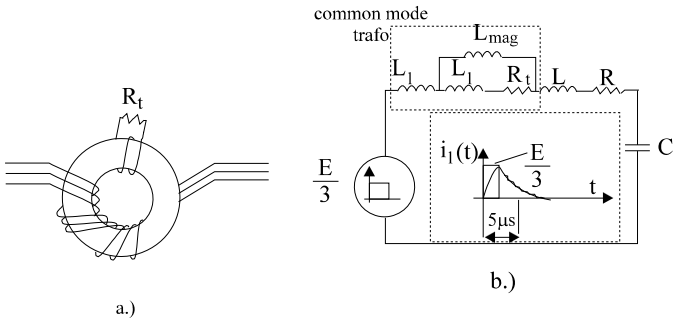

Figure 13.14. a.) common mode trafo, b.) equivalent circuit and leakage current response

The common mode trafo with secondary resistor R_t (L_l – leakage inductance, L_{mag} – magnetizing inductance) reduces the main flux in comparison with the common mode choke. Consequently, the ferrite core size may be reduced notably [10].

Reducing drastically the rms value of the leakage current leads to lowering the risk for incorrect operation of residual current-operated circuit breakers. Implicitly, it reduces, to some extent, the shaft voltage V_{rg} and the bearing currents. It appears, however, that bearing currents still have to be further reduced to avoid premature bearing damage through lubrication film electrostatic breakdown.

13.8. CIRCULATING BEARING CURRENTS

Noncirculating common mode bearing currents occur, as shown in the previous section, as a result of common mode voltage pulses (Figure 13.11).

Recently, an additional bearing current — the circulating component — due to the electrostatic current leaks to the laminated core, due to stator coil sides currents, along the machine stack length: $2\Delta i_a$, $2\Delta i_b$, $2\Delta i_c$, has been discovered (Figure 13.15a [9]).

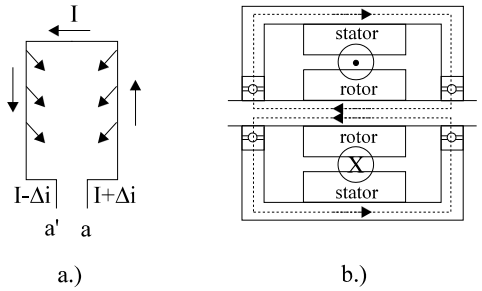

Figure 13.15. a.) current unbalance, b.) net flux and bearing circulating current

These unbalanced longitudinal currents produce a circular net flux that is responsible for an additional, circulating, frame-bearing shaft current.

13.9. REDUCING THE BEARING CURRENTS

Examining the bearing failure in some PWM converter drives after only a few months of operation, bearing fluting (induced by electrical discharge machining (EDM)) has been noted. Bearing fluting manifests itself by the appearance of transverse grooves or pits in the bearing race. The shaft voltage V_{rg} (Figure 13.11) is a strong indication for the presence of bearing currents.

EDM may occur if the electrical field in the thin lubricant film is in excess of 15V (peak)/μm which, for films between 0.2 to 2μm, means 3 to $30V_{pk}$ of shaft voltage, V_{rg}.

Among measures proposed to reduce the shaft voltage V_{rg} and, implicitly, bearing wear we mention here:

- outer-race insulation layer (Figure 13.16a);
- dielectric-metallic Faraday airgap or complete foil (Figure 13.16b) - or paint along full stator length;
- copper-plated slot stick covers (Figure 13.16c);
- one insulated bearing and shaft grounding brush and good motor grounding (to high frequency) from motor to mechanical load and from motor to inverter (drive) — Figure 13.16d [25].

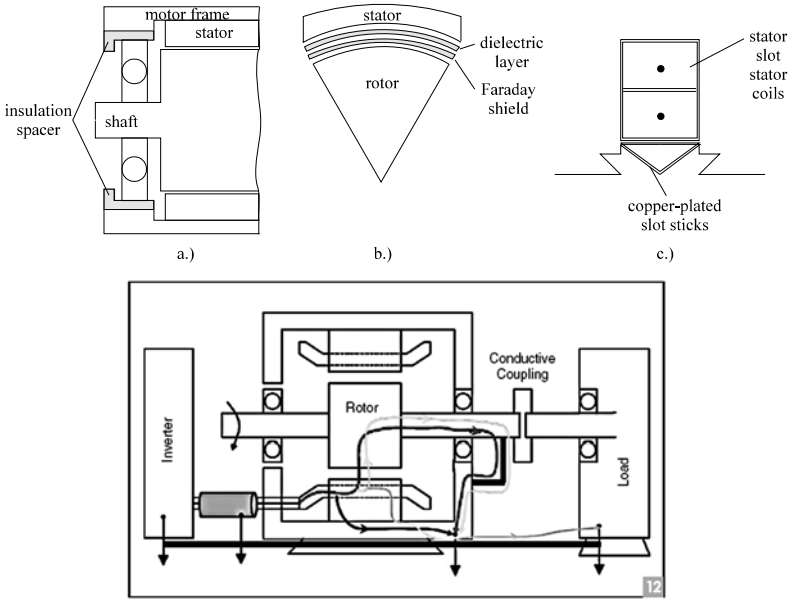

Figure 13.16. Methods to reduce bearing currents: a.) bearing insulation spacer, b.) conduction foil or paint, c.) conduction slot sticks, d.) one insulated and shaft grounding brush and motor, good high-frequency grounding from motor to load and from motor to drive

In fact, all methods introduce a small capacitor in series with the bearing circuit (Figure 13.11) and this is expected to ultimately reduce the bearing currents. The bearing insulation spacer seems to be a must. Only when stator and winding shielding is added - either through conductive foil or paint - is the shaft voltage reduced to less than 5% of its initial value (of the conventional machine) to values of 1-1.2 V(peak). Also, the stator temperature does not change notably due to these conductive shields (in which eddy currents are induced) and thus the methods proposed seem safe

to apply [8]. Finally, when common mode chokes are used (see Section 13.8), the shaft voltage was initially around 30V. After using the full Faraday shield (Figure 13.16b) the shaft voltage was further reduced to less than 1.5V [8].

It is yet to be seen, if the common mode trafo is capable of reducing enough the danger of bearing wear occurrence so as to eliminate or at least reduce the demand for Faraday shields.

13.10. ELECTROMAGNETIC INTERFERENCE

The step change in voltage caused by fast switching IGBTs produces high frequency common mode (Section 13.7) and normal mode currents after each switching sequence in the PWM inverter, due to the parasitic stray capacitors of electric motors.

The oscillatory currents with frequencies from 100kHz to several MHz radiate EMI fields (noises) in the environment, influencing various electronic devices such as AM radio receivers, medical equipments, etc.

A motor model, including stray capacitors and the corresponding common mode and normal mode current paths, is shown in Figure 13.17.

As expected, using a shielded three-core cable (with the shield used as the grounding wire) generally reduces the EMI noise to the limits prescribed through international standards (less than 40dBμV/m).

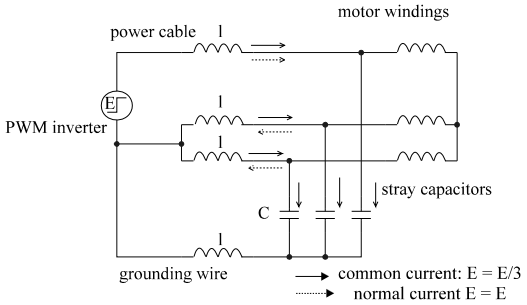

Figure 13.17. AC motor model with stray capacitors

Alternatively, making use of a common mode transformer (Section 13.7) and R_FL_F normal mode filters (Figure 13.18) for the normal mode currents, produces acceptable EMI noise limits with a conventional power cable made through bundling the three feeding wires and the ground wire [11].

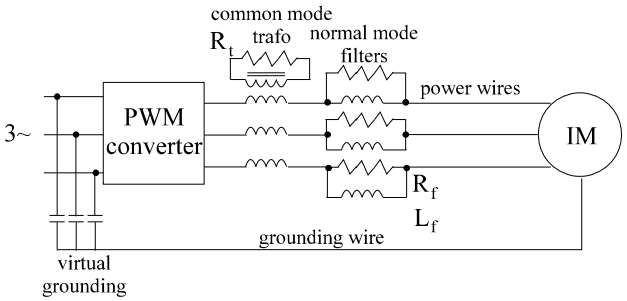

Figure 13.18. EMI reduction through common mode transformer and natural mode filters mounted at inverter output terminals

13.11. THE AUDIBLE NOISE

The audible noise, in fact a part of the EMI spectrum (15 Hz to about 18 kHz), is a main performance index of an electric drive. Audible noise standards, measures to reduce the audible noise in PWM electric drives and methods to measure it (ISO 3340 - 46 standard) constitute a subject of wide interest and debate [12]. In general, the PWM supply in electric drives increases the level of noise related to grid connected electric motors.

Approaches to reduce PWM excited noise include: using an LC filter at motor terminals, changing the switching frequency, operation above 18kHz, use of random PWM [13] or making the PWM drive play music with its noise.

Standards for noise emission of induction motors, for example, are: ISOR 1680, IEC-34-9, NEMA M61-12.49.

13.12. LOSSES IN PWM CONVERTER DRIVES

Losses in PWM converter drives occur both in the motor and in the PEC. The PEC produces current and flux harmonics in the motor and thus additional winding losses and core losses are present in PWM converter drives [14]. The PWM converter losses are of conduction and commutation (switching) types [15].

Though there is a rich literature related to loss modeling in motors and PWM converters, experimental findings are still crucial in view of the complexity of the phenomena. As the switching frequency increases, the PEC losses increase while the motor losses only slightly decrease.

Total drive losses only slightly increase when switching frequency varies from 2 – 10 kHz in a 2 kW motor, for example. Higher power units mean lower switching frequencies; also, it has been shown that if the motor efficiency is high so is PEC efficiency.

A maximum efficiency drive is obtained if the flux increases with torque and there are quite a few control methods to implement it. For vector or DTFC control, adequate flux/torque reference correlation solves the problem rather satisfactorily. However, the speed response, in the first few

milliseconds after a step torque reference increase occurs, is rather slow until the flux in the motor reaches the higher (according to torque reference) levels.

13.13. SUMMARY

- The introduction of a large scale of PWM converter drives with line-side diode rectifiers for powers now up to 500kW per unit and more, has produced considerable progress in energy usage and productivity increases through variable speed.
- However, there are some side effects related to the ultrafast rise time voltage pulses produced by the PWM converter with switching frequency up to 20 kHz sent to the motor often through long power cables, as imposed by application.
- Electromagnetic interference (EMI) is related to conductive (through power source) and electromagnetic voltage radiations at frequencies from 100 kHz to megahertz and produces communication (radio, etc.) damage around or crosstalk in neighboring digital equipment. This aspect is treated extensively in power electronics books although it is by now a field in itself.
- Line current harmonics of 5^{th}, 7^{th}, 11^{th}, … order occur. Limited by demanding international or national standards, they are defined by the total harmonic distortion (THD) factor of harmonic voltages produced in the power source. Passive line filters may solve the problem but care must be exercised to check that filter voltage instabilities do not occur in presence of high performance PWM converter drives.
- If power cables between PWM converter and motor are longer than a critical l_c, which corresponds to one third of voltage pulse rise time t_r (t_r = 0.1-5μs) travel at about half light speed, the voltage is doubled, by reflection, at the motor terminal. This fast high voltage pulse may damage the motor insulation as it stresses initially only the first coils of the stator windings. So it has to be reduced — for cable length $l > l_c$ — by inverter-side low pass filters or by motor terminal filters.
- Increasing the voltage rise time might impede some self-commissioning strategies for motor parameter identification based on step voltage response standstill tests, which are in use for some commercial drives.
- Some PWM strategies may lead to tripling the inverter voltage pulse at motor terminals but special pulse elimination methods may reduce them to the classical double voltage, taken care of as explained above.
- Common mode (zero sequence) voltage pulses occur in the machine and they produce electrostatic leakage currents in the motor — to the frame structure. For such high frequencies a distributed capacitor model of the machine is required. The motor bearing appears also as an elaborate circuit in this case. The common mode stator leakage current may reach the level of the rated current and may impede the action of residual

current circuit breakers and produce notable shaft voltage and bearing currents.

- Common mode chokes and common mode transformers are proposed to reduce the leakage current, shaft voltage and bearing currents. Apparently they are not enough to secure a long life for bearings.
- Current bearing existence is related to rather high shaft voltages (in the order of 5 to 30V peak values); reducing this voltage to 1-2V would reduce the chances for bearing damage caused by electrostatic breakdown of the bearings' 2μm thick film lubricant. This is done through Faraday complete shields (paints) placed along the stator bore and winding end connections, or similar methods.
- The future? It seems to be either to improve existing solutions for curing the side effects of PWM converters or to produce close to sinusoidal input-output converters where all these problems are inherently solved at the price of a more sophisticated converter-motor control and higher costs.

13.14. PROBLEMS

13.1. The line filters: For a PWM converter drive of drive kVA = 25kVA, connected to a grid point with a short-circuit capacity SC kVA = 500kVA, the measured line current harmonics are $i_5 = 25\%$, $i_7 = 5\%$, $i_{11} = 1.5\%$, line harmonics; $f_1 = 60$Hz and line voltage $V_{LL} = 220$V (rms).

Calculate:

13.2. the line current harmonic factor HF;

13.3. the filter capacitor C and inductance L tuned to the 5^{th} harmonic with a detuning factor $\alpha = 0.95$;

13.4. the voltage total harmonic distortion factor THD_f after the filter is introduced.

13.5. The voltage reflection: A PWM converter drive with a rated kVA of 10kVA for maximum phase voltage $V_n = 120$V(rms) at 60Hz has the motor supplied through a power cable with a surge impedance $Z_0 = Z_n/10$ where Z_n is the rated load impedance of the motor. The IGBTs in the PEC have a rising time $t_r = 0.5\mu$s. The electromagnetic wave speed along the cable is $U^* = 160$m/μs.

Calculate:

13.6. the reflection coefficient Γ_m at motor terminals and motor load impedance Z_n for which the reflected voltage is only 20% of DC link voltage;

13.7. the cable critical length l_c;

13.8. for a 20% reflected wave, the required RC filter located at motor terminals.

13.15. SELECTED REFERENCES

1. **S.M. Peeran, C.W.P. Cascadden, "**Application, design and specification of harmonic filters for variable frequency drives", IEEE Trans.vol.IA-31, no.4, 1995, pp.841-847.
2. **J.W. Gray, F.J. Haydock, "**Industrial power quality considerations when installing adjustable speed drive systems", IBID vol.32, no.3, 1996, pp.646-652.
3. **A.M. Walczyna, K. Hasse, R. Czarnecki, "**Input filter stability of drives fed from voltage inverters controlled by direct flux and torque control methods", Proc. IEE, vol.EPA-143, no.5, 1996, pp.396-401.
4. **B. Mollit, J. Allan, "**Stability characteristics of a constant power chopper controller for traction drives", Proc IEE.vol.B, no.1(3), 1978, pp.100-104.
5. **A. von Jouanne, D.A. Rendusora, P.M. Enjeti, J.W. Gray,** "Filtering tehniques to minimize the effect of long motor leads on PWM inverter fed AC motor drive systems", IEEE Trans.vol.IA-32, 1996, pp.919-925.
6. **A.von Jouanne, P. Enjeti, W. Gray,** "Application issues for PWM adjustable speed AC motor drives", IEEE-I.A. magazine, vol.2, no.5, 1996, pp.10-18.
7. **R. Kerkman, D. Leggate, G. Skibinski,** "Interaction of drive modulation and cable parameters on AC motor transients", Record of IEEE-IAS, Annual meeting, vol.1, 1996, pp.143-152.
8. **D. Busse et al, "**An evaluation of electrostatic shielded induction motor: a solution for rotor shaft voltage build-up and bearing current", IBID, vol.I, pp.610-617.
9. **S. Chen, T.A. Lipo, D.W. Novotny,** "Circulating type bearing current in inverter drives", IBID, vol.1, pp.162-167.
10. **S. Ogasawara, H. Akagi,** "Modeling and damping of high frequency leakage current in PWM inverter fed AC motor drive systems", IEEE Trans.vol.IA-32, no.5, 1996, pp.1105-1114.
11. **S. Ogasawara, H. Ayano, H. Akagi,** "Measurement and reduction of EMI radiated by a PWM inverter-fed AC motor drive system", IEEE Trans., vol.IA-33, no.4, 1997, pp.1019-1026.
12. **P. Enjeti, F. Blaabjerg, J.K. Pedersen,** Adjustable speed AC motor drives, application workbook, EPE 1997, Trondheim, Norway.
13. **F. Blaabjerg, J.K. Pedersen, L. Oesterguard, R.L. Kirlin, A.M. Trzynadlowski, S.Logowski,** "Optimized and nonoptimized random modulation techniques for VSI drives", Proc of EPE-95, vol.1, 1995, pp.19-26.
14. **A. Boglietti, P. Ferraris, M. Lazzani, M. Pastorelli,** "Energetic behavior of induction motors fed by inverter supply", Record of IEEE-IAS, Annual Meeting, 1993, pp.331-335.
15. **F. Blaabjerg, U. Jaeger, S. Munk-Nielsen, J.K. Pedersen,** "Power losses in PWM-VSI inverter using NPT or PT IGBT devices", IEEE Trans.vol.IE-10, no.3, 1995, pp.358-367.
16. **I. Abrahamsen, J.K. Pedersen, F. Blaaberg,** "State of the art of optimal efficiency control of induction motor drives", Proc. of PEMC-96, vol.2, 1996, pp.163-170.
17. **F. Abrahamsen, F. Blaabjerg, J.K. Pedersen,** "On the energy optimized control of standard and high-efficiency induction motors in CT and HVAC applications", Record of IEEE-IAS, Annual Meeting, 1997, vol.1., pp.612-628.
18. **D.M. Van de Sype, K. De Gusseme, A.P. Van den Bossche, J.A.A. Melkebeek,** "Sampling algorithm for digitally controlled boost PFC converters", IEEE Trans. Vol. PE – 19, no. 3, 2004, pp. 649-657.
19. **S. Chattopadhyay, V. Ramanarayanan, V. Iayashankan,** "A predictive switching modulator for current mode control of high power factor boost rectifier", IEEE Trans. Vol. PE-18, no. 1, 2003, pp. 114-123.
20. **I. Zhang. F.C. Lee, M.M. Iovanovic,** "An improved CCM single phase PFC converter with a low frequency auxiliary switch", IEEE Trans. Vol. PE – 18, no.1, 2003, pp. 44-50.
21. **S. Chattopadhyay, V. Ramanarayanan,** "Digital implementation of a line current

shapping algorithm for three phase high power factor boost rectifier without voltage input sensing", IEEE Trans. Vol. PE – 19, no. 3, 2004, pp. 709-721.

22. **M. Kazmierkovski, R. Krishnan, F. Blaabjerg,** (editors), Control in Power Electronics, book, Academic Press, New York, 2003.
23. **K. Stockman, M. Didden, F. D'Hulster, R. Belmans,** "Bag the sags" IEEE – IA Magazine, vol. 10, no. 5, 2004, pp. 59-65.
24. **N.Hanigovszki, J. Poulsen, F. Blaabjerg,** "Novel output filter topology to reduce motor overvoltage", IEEE Trans. Vol. IA – 40, no. 3, 2004, pp. 845-852.
25. **M. Fenger, S.R. Campbell, J. Pedersen,** "Motor winding problems caused by inverter drives", IEEE – IA Magazine, Vol. 9, no. 4, 2003, pp. 22-31.